J. Membrane Biol. 42, 375–398 (1978)

Water Exchange across Red Cell Membranes: II. Measurement by Nuclear Magnetic Resonance T_1, T_2, and T_{12} Hybrid Relaxation. The Effects of Osmolarity, Cell Volume, and Medium

Mary E. Fabry and Maurice Eisenstadt

Division of Genetic Medicine, Department of Medicine, Albert Einstein College of Medicine, Bronx, New York 10461

Received 14 November 1977; revised 19 January 1978; revised again 15 May 1978

Summary. We have used the nuclear magnetic relaxation of water protons to measure the diffusional permeability (P_w) of human red blood cells to water as a function of concentration of nonpermeable and permeable solutes. Measurements of T_1, T_2, and a hybrid of the two were made and yielded the same P_w. In the presence of the nonpermeable electrolyte NaCl, membrane permeability is constant between the volumes of 70 and 105 μm^3 and increases both as the cells swell and shrink beyond these limits. Changes in both the internal and external osmolarity, using the permeable solutes urea and ammonium chloride, do not affect membrane permeability. The composition of the suspending medium also has a significant effect on membrane permeability. Cells suspended in plasma have a cell water lifetime about 30 % longer than cells of the same volume suspended in serum, or isotonic saline with human serum albumin. Addition of a crude preparation of fibrinogen in physiological amounts to isotonic saline and human serum albumin restores the cell water lifetime to a value similar to that observed in plasma.

Since the original report of Conlon and Outhred (1972), a number of laboratories have reported measurements of red-cell water permeability by NMR methods (Fabry & Eisenstadt, 1975; Shporer & Civan, 1975; Andrasko, 1976; Benga & Morariu, 1977; Chien & Macey, 1977). Most are based on spin-lattice (T_1) or spin-spin (T_2) relaxation time measurements of water in a Mn(II)-doped medium, but Shporer and Civan (1975) used ^{17}O water relaxation, and Andrasko (1976) used the pulsed field-gradient spin-echo method to measure restricted water diffusion in the red cell. There are large discrepancies between the various methods, especially between cell water lifetimes obtained from T_1 and T_2 of Mn-doped cells (Conlon & Outhred, 1972; Fabry & Eisenstadt, 1975; Benga & Morariu, 1977; Chien & Macey, 1977). With complete experimental

0022-2631/78/0042-0375 $04.80

and theoretical analysis of all ^1H signals in the sample and with judicious use of Mn, we obtain the same water lifetime for T_1, T_2, and T_{12} hybrid (Edzes, 1975) measurements.

The principles of the NMR relaxation method with its advantages of speed and measurement at chemical equilibrium, were discussed by us previously (Fabry & Eisenstadt, 1975) hereafter referred to as (*I*). Briefly, the experiment may be thought of as a measurement of the rate of escape of transiently-labeled water molecules from the cell. The water is "tagged" by changing the direction of the equilibrium nuclear magnetization of its protons. Inside the cell the water protons reorient slowly (about 0.5 sec relaxation time), but we reduce the relaxation outside to about 10 msec by adding small amounts of Mn, typically 2 mM. If the lifetime of cell water is somewhere between these two times, the observed recovery of magnetization comprises a fast component mainly due to relaxation of the plasma water, and a slower component largely determined by the leaving rate of cell water. For relatively low Mn concentrations, of course, the entering rate becomes important, and a complete kinetic analysis of two compartment NMR exchange is needed, as shown below.

The bulk of experimentation on water permeability has involved measurement of the rate of swelling or shrinking under the influence of an osmotic gradient; the results yield unique information but are sometimes difficult to interpret because they involve the simultaneous change of two or more variables. It is somewhat easier to separate the effects of various parameters in experiments at osmotic equilibrium; however, the only non-NMR method available is the isotopic tracer technique of Solomon (1960) and Villegas, Barton and Solomon (1958), which is technically difficult to execute. We report here measurements on the effect of varying the concentration of the permeable solutes urea and ammonium chloride, as well as the nonpermeable electrolyte NaCl, and the composition of the suspending medium on membrane permeability at osmotic equilibrium.

Materials and Non-NMR Methods

Red Cells. For most experiments blood was collected in heparinized Vacutainer tubes and used on the same day. When human serum albumin was to be the ultimate suspending medium, the cells were first washed twice with isotonic NaCl/KCl.

Cell Volumes. Volumes were determined in one of two ways: (i) the total cell volume was obtained from the hematocrit and the number of cells was determined with a Coulter counter, or (ii) the hematocrit was determined and the number of cells was found by

measuring the hemoglobin spectrophotometrically and dividing this number by the mean corpuscular hemoglobin (the hemoglobin content per cell, which is 29 ± 2 μμg/cell for normal subjects (Geigy, 1970)). For cells suspended in plasma, the cell volume was varied by addition of small amounts of water or concentrated salt solution to the plasma. For experiments in an artificial medium, 3 % human serum albumin (HSA) was used; in these experiments the HSA concentration was held constant since it fulfills two roles. It enhances the effect of the Mn(II) on water relaxation, allowing lower Mn(II) concentrations than would otherwise be possible, and it diminishes the extent to which Mn(II) interacts with the membrane, greatly retarding the rate at which Mn(II) can enter the cell. Suitable amounts of NaCl/KCl in the ratio 27:1 were added to achieve the desired cell volume. Cell volumes were measured immediately after the NMR measurements were completed.

Manganese Concentrations. In the measurements reported, $MnCl_2$ was added to the suspending medium to achieve a concentration of 2 mM; packed cells were then added to reach the desired hematocrit. Measurements on the suspending medium, such as T_1, T_2, and osmolarity, were made on supernatant reseparated by centrifugation after equilibration was complete.

Osmolarities. In most cases a Fiske Model III freezing point osmometer was used; for a few determinations a Wescor vapor pressure osmometer was used.

Sedimentation. The rate of sedimentation in erythrocyte suspension depends sensitively on a wide variety of parameters. For relaxation measurements requiring more than a minute, frequent mixing is necessary to prevent the cells from settling. The effect of sedimentation is to make accurate decomposition of the magnetization decay into two components impossible, because the solution contains a distribution of hematocrits.

Osmotic Fragility. Cells were incubated in the desired suspending medium for the time stated and then an aliquot was transferred to a hypotonic solution containing either 46, or 61 mM NaCl/KCl and allowed to hemolyze for 15 min, after which the suspension was centrifuged and the hemoglobin in the supernatant was read as the cyanmet hemoglobin form.

Temperature: The temperature was controlled at 25.0 ± 0.5 °C in all experiments.

NMR Measurement and Theory

Measurement of membrane permeability by NMR relaxation is a general and very sensitive technique; however, it is subject to systematic errors from several sources which we will consider in some detail in the following two sections.

NMR relaxation can be described in terms of two lifetimes, T_1 and T_2. T_1 is the characteristic time for loss of energy to the environment or lattice, and is known as the spin-lattice or longitudinal relaxation time. T_2 is characteristic of the rate at which spins exchange energy among themselves, and is known as the spin-spin or transverse relaxation time. Although many interactions leading to relaxation contribute equally to

T_1 and T_2, each mode also has unique mechanisms of relaxation. Both can be used to measure membrane permeability; however, when this is done, the resulting cell water lifetimes obtained by the two methods do not agree (Benga & Morariu, 1977; Chien & Macey, 1977). We found a similar effect, where the largest disagreement (about 20 %) was observed at small cell volumes and the discrepancy between the two techniques disappeared at high cell volumes. The difference is almost entirely due to spin-diffusion, which is discussed in greater detail elsewhere (Eisenstadt & Fabry, 1978). Briefly, spin diffusion is a strictly NMR phenomenon, which results in the T_1 relaxation rates of the protein and water protons mixing by spin exchange, much as the relaxation rates of water protons inside and outside the cell mix via water exchange. The effect of spin diffusion on the measured T_1 decay constant, ϕ_{1-}, is to make it slower, which in turn makes k_x^{-1}, the cell water lifetime, appear longer.

It is possible to quantitatively account for spin diffusion effects. To see how this may be done, we will first outline the derivation of an exact solution to T_2 relaxation and illustrate how it may be extended to accomodate spin-diffusion in the T_1 mode; further descriptions of NMR relaxation techniques are in the *Appendix*.

Consider a red cell suspension, shown symbolically in Fig. 1. Phase A is exchangeable cell water, B is the exchangeable plasma (or other media) water, and F and G are the volumes of nonexchanging protons, mainly

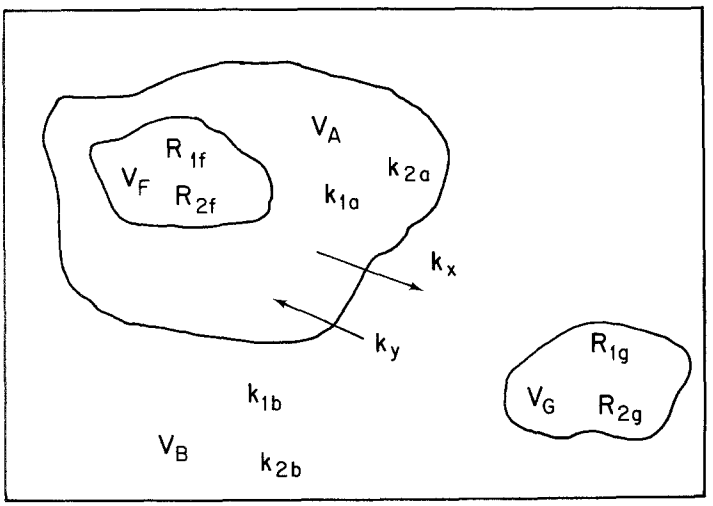

Fig. 1. Symbolic representation of blood cell suspension. V_A and V_B are volumes of exchangeable water in cells and suspending medium; V_F and V_G are volumes of nonexchangeable protein-protons in cells and medium. Rates are defined in text

due to the 35 % hemoglobin concentration in the cell, and as much as 7 % serum proteins outside. Let the T_1 and T_2 rates in each exchanging phase be k_{1a}, k_{2a}, k_{1b}, and k_{2b}, and corresponding nonexchanging rates be R_{1f}, R_{2f}, R_{1g}, and R_{2g}. The probabilities per second of a water molecule leaving A or B are k_x and k_y, respectively. We assume these rates are the same for all molecules in one phase, i.e., no diffusion limitations (*I*). Since the NMR experiment is done at chemical equilibrium, k_x and k_y are related:

$$k_x N_A = k_y N_B \tag{1}$$

where N_A and N_B are the total numbers of exchangeable protons in volumes V_A and V_B, and we define similar quantities N_F and N_G for the nonexchanging protons. In all of what follows, we assume the thermal equilibrium magnetization in each phase, M_A^0, M_F^0, etc., is directly proportional to the corresponding N_A, N_F, so we use them interchangeably.

First, consider a pure T_2 experiment. At $t=0$, the total M^0 is rotated into the $x-y$ plane, and the echoes begin to decay toward zero. The loss of transverse magnetization in the A phase occurs through inherent T_2 processes (k_{2a}) as well as transfer into the B phase (k_x). It also gains magnetization from the B phase (k_y). We assume dephasing due to chemical shifts is negligible. Nonexchanging contributions such as M_F simply decay at the rate R_{2f}. These can all be described by the rate equations

$$\begin{aligned} dM_A/dt &= -(k_{2a}+k_x)M_A + k_y M_B \\ dM_B/dt &= +k_x M_A - (k_{2b}+k_y)M_B \\ dM_F/dt &= -R_{2f} M_F \\ dM_G/dt &= -R_{2g} M_G. \end{aligned} \tag{2}$$

The solutions for $M_F(t)$ and $M_G(t)$ are simple exponentials,

$$\begin{aligned} M_F(t) &= M_F^0 \exp(+R_{2f} t) \\ M_G(t) &= M_G^0 \exp(-R_{2g} t). \end{aligned} \tag{3}$$

The pair of coupled differential equations in Eq. (2) have the general solution

$$\begin{aligned} M_A(t) &= A_{2+} \exp(-\phi_{2+} t) + A_{2-} \exp(-\phi_{2-} t) \\ M_B(t) &= B_{2+} \exp(-\phi_{2+} t) + B_{2-} \exp(-\phi_{2-} t), \end{aligned} \tag{4}$$

where

$$2\phi_{2\pm}=(k_{2a}+k_{2b}+k_x+k_y)\pm[(k_{2a}-k_{2b}+k_x-k_y)^2+4k_xk_y]^{\frac{1}{2}}. \quad (5a)$$

and the amplitudes are given by

$$\begin{aligned}
(\phi_{2+}-\phi_{2-})A_{2+}&=(k_{2a}+k_x-\phi_{2-})M_A^0-k_yM_B^0\\
(\phi_{2+}-\phi_{2-})A_{2-}&=(\phi_{2+}-k_{2a}-k_x)M_A^0+k_yM_B^0\\
(\phi_{2+}-\phi_{2-})B_{2+}&=(k_{2b}+k_y-\phi_{2-})M_B^0-k_xM_A^0\\
(\phi_{2+}-\phi_{2-})B_{2-}&=(\phi_{2+}-k_{2b}-k_y)M_B^0+k_xM_A^0.
\end{aligned} \quad (5b)$$

These equations are used in the analysis of CPMG data below. The measured echo height at time t is the sum of $M_A(t)$, $M_B(t)$, $M_F(t)$, and $M_G(t)$. ϕ_{2+} and ϕ_{2-} are the measured fast and slow decay constants. The intercept, H, of ϕ_-, the slowly decaying component, [Eq. (6) in *I*] may be derived from Eq. 5b.

To introduce spin diffusion into T_1 relaxation, we write rate equations analogous to Eq. 2, with M defined as deviations from M^0:

$$\begin{aligned}
dM_A/dt&=-(k_{1a}+k_x+k_t)M_A+k_yM_B+k_sM_F\\
dM_B/dt&=k_xM_A-(k_{1b}+k_y)M_B\\
dM_F/dt&=k_tM_A-(R_{1f}+k_s)M_F\\
dM_G/dt&=-R_{1g}M_G.
\end{aligned} \quad (6)$$

New terms have been added to the first and third lines of Eq. (2) to yield Eq. (6). The new spin exchange rate constants, k_s and k_t, are defined analogously to k_x and k_y, and can be estimated from independent experiments similar to those described by Eisenstadt and Fabry, 1978. Exchange with plasma proteins can be neglected. The general solutions given by Eq. (4) become three magnetizations, each of which is the sum of three exponentials with the three exponents being roots of a cubic equation; an exact solution for the amplitudes was also obtained. These equations will be described in more detail elsewhere. The net result is a modification of our previous treatment, which considered relaxation of protein protons as an independent process. The curve-fitting procedure is otherwise the same.

The choice of which relaxation method to use is somewhat arbitrary. The conventional T_1 method has great experimental simplicity, placing minimal demands on phase and pulse settings and magnetic field stability. It was the method we originally used (*I*) and still used for much of

the work presented here, but it suffers from two defects: slow data collection rate, and the complexities of treating the slowly relaxing protein-protons, which eventually dominate the magnetization decay in the third decade.

A T_2 measurement can be obtained in one scan, and T_2 for protein protons is very short, so the asymptotic slope is solely the slow component, ϕ_{2-}, in Eq. (5). There is a large Mn-induced chemical shift between the cell and plasma water (Frait, Fraitora & Doskocilova, 1973). This was once thought by ourselves and others (Chien & Macey, 1977) to be a defect of the T_2 method, but this is not so. Because of the random nature of exchange, water protons leaving the cell are both dephased randomly and relaxed by the inherently random T_2 process. Both processes lead to magnetization decay, and both are proportional to Mn^{++} concentration; from the known chemical shift and T_2, the latter dominates at any Mn^{++} concentration. Woessner (1960) gives graphs for quantitative evaluation. On the negative side, pulse and phase adjustments are rather critical, error compensation is not outstanding even with the MG modification (Meiboom & Gill, 1958), and magnetic field fluctuations are onerous.

The hybrid method arose from a desire to measure T_1 in one scan just as T_2, resulting in a great time saving compared to point by point data collection typical of T_1 measurements. The hybrid method is described in the *Appendix*. Hybrid T_{12} measurements show the same desirable features as T_2, provided the relative amount of time spent in the T_2 domain keeps the protein T_{12} much shorter than Φ_-^{-1}. Demands on stability seem less than for T_2, and for most multiplet sequences, error compensation is excellent (Edzes, 1975). The added complexity is purely algebraic and is no problem once it is programmed. Curve fitting procedures are the same for T_2 and hybrid data. Hybrid relaxation is our current preferred method.

Data Analysis

The decomposition of two exponentials is a notoriously difficult task, since, in general, the curve-fitting process involves three parameters: two exponentials and their relative amplitudes. If the relative amplitudes are not known, it is frequently possible to fit the same set of data points with several different combinations of fast and slow exponentials. The fast exponential can be neglected in the case of water exchange only when

high concentrations of Mn(II), which may be physiologically perturbing, are used. To extract an accurate value of cell water lifetime from magnetization decay, it is desirable to keep k_x as the only adjustable parameter in curve fitting, therefore several ancillary measurements must be included. In addition to H_t and the hemoglobin concentration discussed above, the relaxation times of water protons in cells and doped plasma as separate phases are needed. The first is measured in packed cells for various cell volumes. T_1 is quite long compared to the cell water lifetime. As is discussed elsewhere (Eisenstadt & Fabry, 1978), the measured T_1 is a combined relaxation of hemoglobin and water protons, so care must be taken in carrying over this result to the doped plasma case. This is only a serious problem for pure T_1 experiments, discussed above. For hybrid experiments, it suffices to assume the apparent packed cell T_1^{-1} as k_{1a}, and use the two-phase calculation in the *Appendix*.

T_2 of water in packed cells is much shorter than T_1, and can introduce a discrepancy in lifetimes if ignored; in fact, in the limit of high Mn (fast plasma relaxation), ϕ_{2-} is exactly $k_{2a}+k_x$ [Eq. (5)]. We measured cell water T_1 and T_2 as a function of volume, Fig. 2, which gave the needed k_{1a} and k_{2a} for all of the experiments reported here.

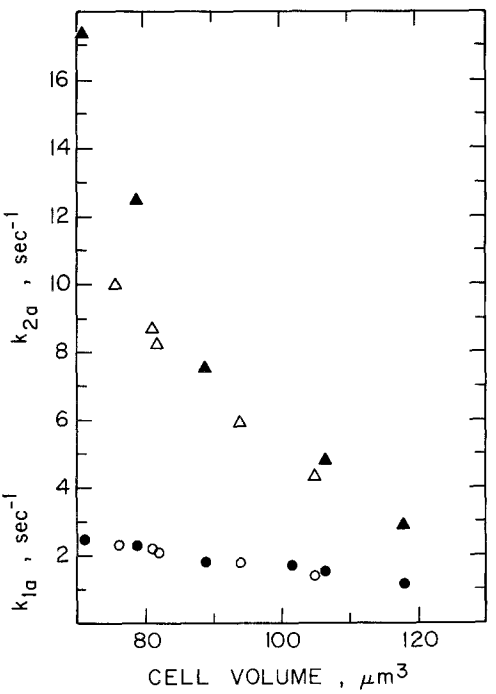

Fig. 2. T_2 and apparent T_1 of water protons in undoped packed red cells *vs.* cell volume. ○: k_{1a} ($\equiv T_{1a}^{-1}$), 25 MHz; ●: k_{1a}, 20 MHz; △: k_{2a} ($\equiv T_{2a}^{-1}$), 25 MHz; ▲: k_{2a}, 20 MHz

The relaxation rates in doped plasma alone, k_{1b} and k_{2b}, enter strongly into the calculation, and vary slightly from sample to sample depending on how much Mn is added, so they are measured for each sample. They are fast, single exponential decays, so measurement is rapid. It is possible that Mn(II) could bind to the cell membranes and change the values of k_{1b} and k_{2b} from those measured in cell-free solutions. We have made a detailed study of relaxation at constant k_{1b} and a wide range of hematocrits (I) (i.e., the ratio of extracellular volume to membrane area was varied). We found that all data could be consistently described in terms of a single water exchange time and a single k_{1b} determined from a cell-free measurement. This would not be possible if there were an appreciable contribution from Mn(II) bound to membranes since this would cause measurements at high hematocrit to deviate from the curves calculated from theory. We do not have such complete data for T_2; however, since the results of T_1 and T_2 experiments are consistent [*see* Figs. (5) and (6)], we conclude that membrane bound Mn(II) does not have a significant effect on T_2 either.

It is necessary to correct for protein-proton relaxation in order to include the first three or four points in the data fitting for the CPMG and hybrid methods. T_1 of protein-protons is also greatly affected by spin transfer with cell water, but for correction of hybrid relaxation, it again suffices to use an apparent T_1, because the short protein T_2 dominates the protein spin behavior. Its T_2 is definitely not a single exponential, and is probably a distribution. For correction purposes, we use an average value, weighted according to signal gate width, based on careful measurements of both free induction decays and spin-echo trains of red cells in H_2O and D_2O. We have shown that we are observing all of the protein-protons by T_2 measurements on cells well equilibrated with a 10 % H_2O-90 % D_2O mixture.

The apparent protein T_1 is measured in a high hematocrit sample with heavily doped plasma, such that water protons are rapidly relaxed, leaving a long decay largely due to protein-protons, e.g., Fig. 1 of *I*. Its slope is shown in Figure 3, for 20 and 25 MHz, as a function of cell volume. It always showed single exponential behavior. An average T_2^{-1} is also shown in Fig. 3, suitable to our experimental NMR parameters. Plasma protein concentration is so low, and its relaxation so much faster than the Hb because of the Mn, that we ignore it completely in relative signal amplitude corrections. For volume corrections (below), it is included.

For pure T_1 experiments, a three-phase exchange calculation (includ-

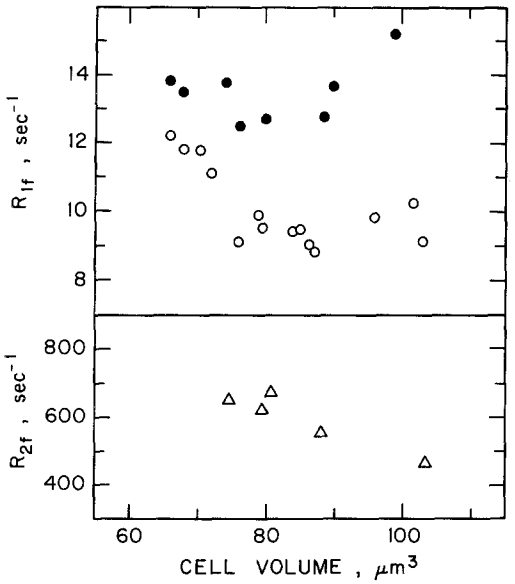

Fig. 3. Average T_2 and apparent T_1 of hemoglobin protons in red cells suspended in HSA-H_2O solution. $R_{1f}(\equiv T_{1f}^{-1})$ obtained in heavily doped medium, $R_{2f}(\equiv T_{2f}^{-1})$ in undoped medium. ○: R_{1f}, 25 MHz; ●: R_{1f}, 20 MHz; △: R_{2f}, 25 MHz

ing cell water protons, extracellular water protons, and protein protons) was necessary to account for spin diffusion effects; otherwise systematic errors arose which ranged from as little as 5 % for cell volumes over 100 μm^3 up to 20 % for cell volumes under 70 μm^3. A two-phase calculation (cell water and extracellular water protons, only) is accurate to better than 10 % in determining slopes, but introduces serious errors in the amplitude of the slowest component in the doped plasma case. As with any type of exchanging system, spin *or* molecular, the amplitudes of the exponential components are no longer proportional to the spin populations in each phase. As exchange rates become comparable to the relaxation rates of the separate phases, the slowest component begins to dominate the observed relaxation. Methods of obtaining the necessary spin transfer rates have been described elsewhere (Eisenstadt & Fabry, 1978). When curve fitting with three-phase formulas are used, all three methods give the same k_x to ± 10 %.

The remaining parameter needed is k_y/k_x, obtained from Eq. (1) and the measured H_t and cell volume. The nonexchanging volume is determined primarily by the volume of hemoglobin and possibly some water of hydration. The relevant value depends to a large degree on the time scale of the experiment (Kuntz & Kauzmann, 1974). For us,

any hydration water with a lifetime $\gg 20$ msec is considered nonexchanging. We can determine the excluded volume from our own data, by comparing the measured Φ_- for a series of samples covering a wide range of hematocrit. For low H_t, k_y is very small, Eq. (1), and Φ_- is independent of excluded volume. For high H_t, $k_y > k_x$, so an excluded volume can be derived to give a k_x independent of H_t. We obtain 22 μm^3, independent of cell volume.

Equation (1) expressed in terms of excluded volume fractions and measured hematocrit is

$$k_y = k_x(1-\alpha)H_t/(1-\beta)(1-H_t), \tag{7}$$

where

$$\alpha = V_F/(V_A+V_F), \qquad \beta = V_G/(V_B+V_G), \tag{8}$$

the fraction of excluded volume in the cells and plasma, respectively.

No elaborate curve-fitting procedures are used to extract k_x from the raw data. Using all of the known parameters above, we calculate the decay curve, Eq. (5*a*) for T_2 or Eq. (A6) for T_{12} for several likely values of k_x. The fractional slow (Φ_-) component is calculated for the first few points, where it differs significantly from unity because of the fast component and the Hb relaxation. These depend on the choice of k_x, so a family of corrected points are obtained. Then the best straight line is drawn through the asymptote and one set of corrected points. The slope Φ_- determines a unique k_x and should match the corrected early data points for that k_x. They generally do, but sometimes small adjustments in slope are made. Since we have over two decades of linear decay, the asymptote alone would give reasonable values of k_x, but for better than 10% accuracy, it is important to know where the faster components can be neglected, as well as picking up a few more points to fit a single exponential.

Usually the asymptote remains a pure exponential well into the third decade, and cell-water lifetime determined by T_{12} and T_2 methods agree to $\pm 5\%$ for any given sample, provided the spectrometer is well adjusted. Figure 4 shows an example of two T_{12} hybrids with different spacing, and a T_2, all measured on one sample of cells at high salt concentration, hematocrit .30, cell volume 67 μm^3. Values of cell-water lifetime are 10.0, 9.5, and 11.0 msec, respectively. Each decay curve consisted of 200 scans at 1 sec each. The best set of corrected data for the first few gates is also shown. The small inset graphs of calculated Φ_-^{-1} *vs.* k_x^{-1} give a good idea of the accuracy, and are also used to read off the final choice of k_x.

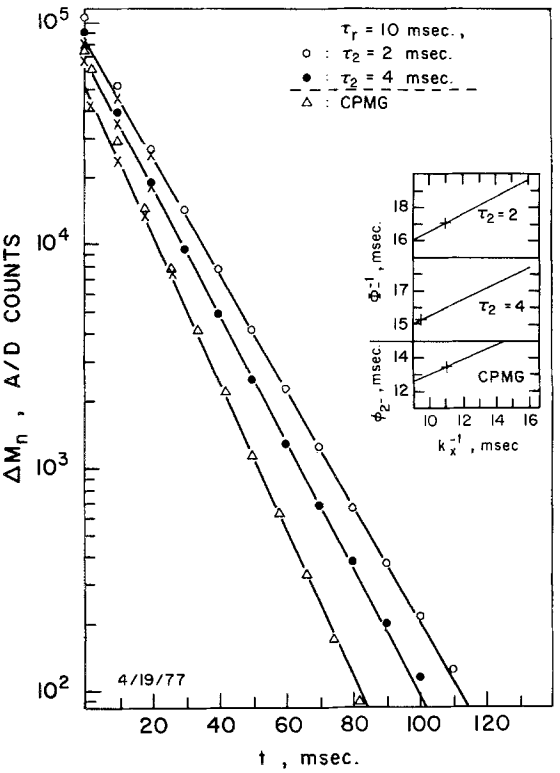

Fig. 4. Determination of cell-water lifetime k_x^{-1} for red cells suspended in NaCl/KCl/HSA, $H_t = 0.30$, cell volume 67 μm^3. Data taken with two different hybrids, and one CPMG experiment, with $t_{cp} = 5$ msec, and a half-gate on the initial FID. Data corrected for fast Φ_+ component and Hb signal denoted by x. Insets show theoretical curves of slow component slope Φ_-^{-1} *vs.* k_x^{-1}. Best fit for k_x^{-1} shown by +

Results and Discussion

The parameter measured in these experiments is the cell water lifetime, k_x^{-1}, which is related to the half-life for water exchange by $t_{1/2} = 0.693\, k_x^{-1}$. In turn, k_x^{-1} is related to P_w, the permeability to water in the absence of an osmotic gradient, by the equation (Stein, 1967)

$$P_w = 10^{-4} k_x (V - V_F)/A, \quad \text{cm sec}^{-1}. \tag{9}$$

Where V is the measured cell volume in μm^3, V_F is the excluded volume in μm^3, A is the area of the cell in μm^2, and k_x is in sec^{-1}. For this calculation $A = 163$ μm^2 was used (Geigy Handbook, 1970). Two approaches have been used to estimate V_F: (i) A value of 22 μm^3 per cell

can be calculated from the hemoglobin content per cell and the density in g/ml of hemoglobin. Measurement of the water content of the red cell by dehydration of a known volume of packed cells yields a similar value (Dick, 1971). (ii) A quantity often referred to as the excluded volume, or b, can be estimated from measurements of the red cell volume as a function of osmotic pressure; b is the apparent excluded volume required to make a red cell behave as a perfect osmometer. It is greater than the volume of 22 μm^3 occupied by hemoglobin and generally is in the range of 30–50 μm^3 (Dick, 1971). More correctly, this value should be thought of as a correction for the volume occupied by hemoglobin plus a term reflecting the chemical activity of the cellular constituents. Since we are interested in the amount of water that can exchange on a time scale determined by the red cell membrane permeability, 15–20 msec, the osmotic b value is not suitable for our purposes. As discussed in the previous section, we determine an excluded volume of 22 μm^3 from our own NMR relaxation measurements, equal to the minimum excluded volume.

P_w as a Function of Cell Volume for Cells Suspended in Heparinized Plasma and in NaCl/KCl/HSA

We have chosen to present the data both as a function of k_x^{-1}, the cell water lifetime, which is the experimentally determined parameter, and as P_w, because, although P_w is a more universal parameter, it is also more derived and gives one a less accurate picture of the experimental error. Figures 5 and 6 show the effect of cell volume on k_x^{-1} and P_w, respectively, for cells suspended in heparinized plasma. P_w increases as cell volume increases, but the measured values are not, in general, reproducible. Measurements at a fixed cell volume but with variable hematocrit or T_{1b} do result in a consistent value of k_x^{-1} for a given sample, so that the irreproducibility seems to be associated with the membrane rather than the measurement technique.

Also shown in Figs. 5 and 6 is the variation in k_x^{-1} and P_w for cells suspended in 3% HSA and variable amounts of NaCl/KCl. The measured permeabilities in this case are very reproducible. The T_1 results plotted in Figs. 5 and 6 were collected over the past three years and are in excellent agreement with the T_2 and T_{12} data collected in the past year. We find that membrane permeability is approximately constant between cell volumes of 70 and 105 μm^3 (the cell volume for an isotonic

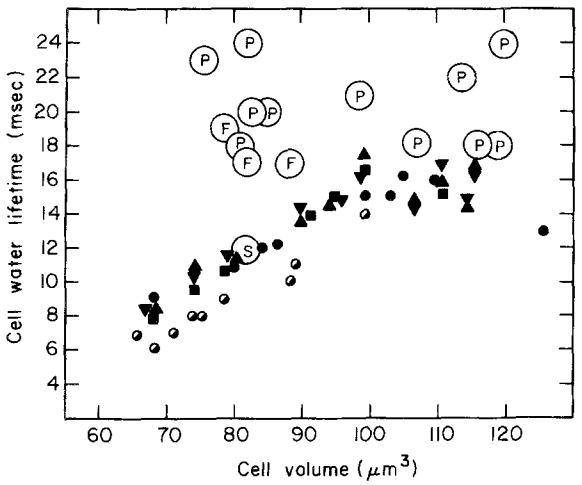

Fig. 5. Cell water lifetime (k_x^{-1}) *vs.* cell volume at 25 °C; most data taken at 25 MHz. Ⓟ: cells suspended in plasma; Ⓕ: cells suspended in HSA with added fibrinogen; Ⓢ: cells suspended in serum. Other symbols are for cells suspended in HSA/NaCl/KCl: ●, T_1; ■, T_2; ▼, ▲, T_{12}; ◪ T_1 taken at 20 MHz

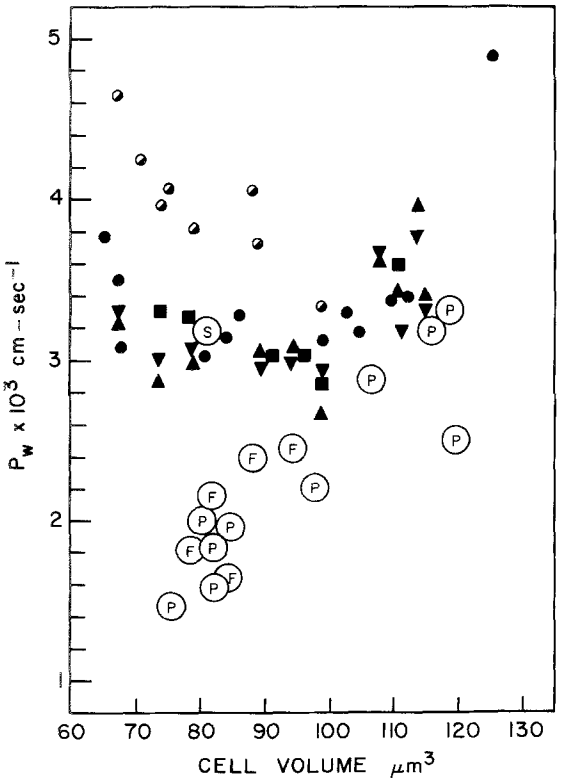

Fig. 6. Data from Fig. 5 replotted as membrane permeability $P_w = (k_x)\ (V - V_F/A) \times 10^{-4}$ cm sec^{-1}, where $V_F = 22$ μm^3 and $A = 163$ μm^3. Ⓟ: cells suspended in plasma; Ⓕ: cells suspended in HSA with added fibrinogen; Ⓢ: cells suspended in serum. Other symbols are for cells suspended in HSA/NaCl/KCl. ●, T_1; ■, T_2; ▼, ▲, T_{12}; ◪, T_1 taken at 20 MHz

solution is about 85 μm^3) and increases both as the cells shrink below 70 and swell above 105 μm^3.

Villegas *et al.* (1958) concluded from their data that the membrane permeability decreased when the cell volume increased. Outhred and Conlon (1973) concluded that the product $P_w A$ remains constant as the cells swell. Both studies covered a smaller range of cell volumes than ours.

P_w in the Presence of the Permeable Solutes Urea and Ammonium Chloride

Figure 7 shows membrane permeability as a function of osmolarity for cells suspended in NaCl/KCl/HSA, and cells suspended in the same medium with added urea and ammonium chloride. Since both urea and ammonium chloride are permeable solutes, the cell volume is largely determined by the concentration of the impermeant cation sodium. Somewhat swollen cells were chosen because it seemed likely that they would be most sensitive to concentration effects. These results, which represent data for a constant cell volume of 105 ± 5 μm^3, are shown in Fig. 7. Membrane permeability seems relatively insensitive to the addition of urea up to 0.6 M and NH_4Cl up to 0.35 M. Both solutes

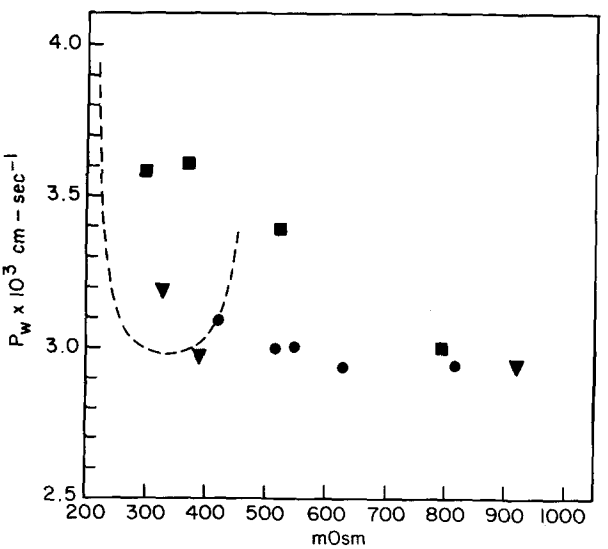

Fig. 7. Membrane permeability *vs.* osmotic strength of the suspending medium. Cell volume constant (105 ± 5 μm^3) determined by NaCl concentration. ●, urea added; ■, NH_4Cl, pH 7.6, added; ▼, NH_4Cl, pH adjusted to 7.1

penetrate the membrane and result in high concentrations inside the cell as well as outside. Chien and Macey (1977) reached a similar conclusion on the effect of urea under different experimental conditions. The results suggest that, in the absence of strong, specific interactions, ionic strength and solute concentrations have little effect on membrane permeability.

The Origin of the Difference in Permeability Beween Cells Suspended in Heparinized Plasma and Cells Suspended in NaCl/KCl/HSA

A number of possible causes of this permeability difference were tested. Azide, in the concentration used as a preservative in HSA, was added to cells suspended in HSA and plasma, respectively. The concentration of HSA itself was varied from zero to three times its physiological concentration in plasma, and heparin was added to it. Physiological concentrations of Ca^{++} and Mg^{++} were tested. Membrane permeability was unaffected by these changes. The pH was also varied from 6.9 to 8.0 by addition of CO_2 and HCO_3^-; for a given cell volume the membrane permeability was not affected by pH.

Membrane permeability determined in serum was found to be equal to that observed in NaCl/KCl/HSA solutions. This surprising result suggested that the difference in permeability was due to one of the proteins in Cohn fraction I. When crude fibrinogen was added to NaCl/KCl/HSA, the membrane permeability decreased to values more like those observed in plasma. The results are shown in Figs. 5 and 6. When the concentration of fibrinogen added exceeds that in normal plasma by a factor of about three, aggregation of the red cells is observed; the effect of this on permeability is yet to be determined.

An alternative interpretation of these observations would be that aggregation occurs in plasma and leads to an apparent decrease in permeability. However, aggregation seems an unlikely explanation because our observed permeability is not a function of hematocrit (*I*), whereas aggregation would be expected to be (Chien, 1975). Also, in the absence of Roleau formation, the area of contact between aggregated cells is small, and would not be expected to significantly affect the diffusion of water.

The Effect of Mn(II) on the Red Cell Membrane

Our original studies suggested that at concentrations above 5 mM Mn(II) in plasma, the red cell permeability to water increased. We will use

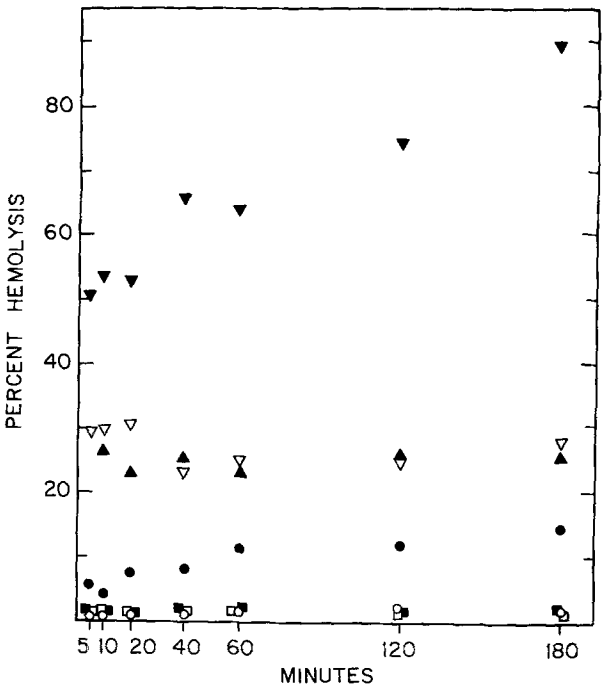

Fig. 8. Percent hemolysis of cells subjected to an osmotic challenge in 46 mM NaCl/KCl, following incubation for the indicated times in the indicated suspension medium: ■, 2 mM Mn(II) in plasma and □ its control; ●, 20 mM Mn(II) in 3 % HSA and isotonic NaCl/KCl and ○ its control; ▼, 20 mM Mn(II) in isotonic NaCl/KCl; ▲ 2 mM Mn(II) in isotonic NaCl/KCl; ▽, the control for the preceding two. The controls have no Mn(II)

osmotic fragility to demonstrate that Mn(II) concentrations below 2 mM in plasma or 3 % HSA (such as those used in our experiments) do not affect membrane properties, and explore the effects of high Mn(II) concentrations (above 10 mM). The rate at which water passes through the membrane at osmotic equilibrium has no direct effect on the osmotic fragility of cells exposed to hypotonic media; however, a substance which alters the membrane response to one probe may also alter it to another and osmotic fragility appears to be a suitable alternate probe which allows independent study of the effect of Mn(II) on membranes.

Figure 8 shows the effect of 2 and 20 mM Mn(II) on the hemolysis of cells subjected to an osmotic challenge after various periods of exposure to Mn(II). The control solutions, which contain no Mn(II), show very little hemolysis when challenged with 46 mM NaCl/KCl. Solutions containing 2 mM Mn(II) show no deviation from the control when HSA or plasma are present, even after three hours incubation with Mn(II). Cells suspended in

isotonic NaCl/KCl are inherently more fragile than cells in HSA or plasma, but the addition of 2 mM Mn(II) does not increase their fragility. However, exposure to 20 mM Mn(II), even for periods as short as 5 min, increases the percent hemolysis from 25 to 50%. The effect of 20 mM Mn(II) is considerably less when 3% HSA is present; nevertheless, fragility is increased and, as in the saline-only case, the percent hemolysis increases as the length of exposure increases.

Another effect of high Mn^{++} concentrations on the apparent membrane properties should be noted. 50 mM $MnCl_2$ alone results in a solution of 150 mosmol; if the suspending medium was isotonic (300 mosmol) prior to the addition of Mn^{++}, the cell volume following addition of Mn^{++} will be about 65 μm^3. For such cells, T_{2a} decreases from its isotonic value of about 150 to about 50 msec, the volume of exchangeable water decreases, and spin exchange increases.

Conclusions

In heparinized plasma, isotonic red cells are found to have a membrane permeability, P_w, of $2.1 \pm 0.2 \times 10^{-3}$ cm-sec^{-1}. Increasing the cell volume above 85 μm^3 results in erratic variations of P_w. If the cells are suspended in NaCl/KCl/HSA, the measured P_w is reproducible and constant for cell volumes between 70 μm^3 and 105 μm^3. Membrane permeability increases for cells with volumes below 70 and above 105 μm^3. Below 70 μm^3 the cells are crenated; these echinocytes are characterized by protuberances which may have different membrane properties, such as locally higher permeabilities. Above 105 μm^3 it is possible that the approximation of constant membrane area as the cell volume increases may begin to break down. Alternatively, the increased P_w may simply reflect the onset of membrane instability prior to hemolysis. In this system, the hemolytic volume is about 130 μm^3, and the membrane permeability observed for cells with a volume of 125 μm^3 is very high. The addition of the permeable solutes urea, up to 0.6 M, and NH_4Cl, up to 0.35 M, has little effect on membrane permeability. Since these solutes increase concentrations inside the cell as well as outside, we conclude that it is cell volume or perhaps cell configuration which determines membrane permeability in swollen and shrunken cells, rather than the osmolarity of the internal or external medium.

Although P_w is more reproducible in NaCl/KCl/HSA, it increases by 30% to $3.0 \pm 0.2 \times 10^{-3}$ cm sec^{-1}, due to the absence of one of the

constituents of Cohn Fraction I, probably fibrinogen. The observation that fibrinogen decreases membrane permeability to water and possibly influences the permeability as cells swell suggests that fibrinogen may bind to the outside of the cell membrane and play a stabilizing role analogous to that proposed for spectrin, which binds on the inside of the membrane (Steck, 1974).

Manganese in high concentrations (over 10 mM) was found to increase membrane permeability to water, and also the susceptibility to hemolysis when the cells are subjected to osmotic challenge. Plasma and HSA minimize the effects of Mn(II) on the membrane, presumably by complexing with it.

The cell water lifetimes reported here were measured by pure T_1, pure T_2, and a hybrid T_{12} technique. Differences between k_x values derived from T_1 and T_2 measurements on the same sample were traced to spin diffusion effects (Eisenstadt & Fabry, 1978). For a given sample, all measurement techniques now result in a single value of k_x.

This work was supported by N.I.H. grant HL-17571, American Cancer Society Institutional Grant IN-28-0. We thank G. Neumann for making the osmotic fragility measurements.

Appendix

We obtain the cell water lifetime from three distinct types of relaxation measurement: (i) T_1, by the $180°-\tau-90°$ pulse sequence; (ii) T_2 by the CPMG (Carr & Purcell, 1954; Meiboom & Gill, 1958) spin-echo method; (iii) T_{12} hybrid relaxation (Edzes, 1975). All of them amount to disturbing the thermal equilibrium magnetization of the water protons and following the rate at which it approaches a final, constant value, which may or may not be the equilibrium value. We discuss their characteristics:

1) The magnetization is inverted from its equilibrium direction along the magnetic field ($+z$) to the $-z$ direction by a 180° radiofrequency (RF) pulse. Thereafter the magnetization shrinks to zero and begins to build up in the $+z$ direction. Its magnitude is sampled at some time τ by applying a 90° pulse, and measuring the size of the free-induction decay (FID). This is repeated for various τ, and a complete magnetization recovery curve is obtained.

2) The CPMG method consists of rotating the magnetization from the $+z$ direction into the x-y plane with a 90° RF pulse, and then applying a sequence of 180° pulses. After the 90° pulse, the magnetization precesses about the field direction axis at the Larmor frequency. But the frequency

varies over the sample due to field inhomogeneities, and the detected signal (FID) decays due to phase cancellation in a few milliseconds. The sole purpose of the 180° pulses is to repeatedly refocus the signal (spin-echos), which is possible because the dephasing is coherent. But the echos do decay to zero due to incoherent relaxation processes, with a characteristic time T_2.

3) The hybrid method arose from a desire to measure T_1 in one scan just as T_2, resulting in a great time saving compared to 1. In the older method, the 90° sampling pulse disturbs the magnetization recovery, since while it is in the x-y plane it is decaying to zero with time constant T_2. But if the sampling time is kept much shorter than T_2, a $(-90°)$ pulse can restore the magnetization to the z direction with little disturbance. This can then be repeated many times to sample the complete recovery. Actually a simple 90°-$(-90°)$ doublet leads to cumulative errors and it is better to use a 90°-$(-180°)$-90° triplet or even a quartet (Edzes, 1975), but the principle is the same. However, the condition of negligible T_2 decay during the multiplet is very restrictive, particularly since the effect of T_2 accumulates, the more samples taken in a given time. But Edzes (1975) has pointed out that this decay can easily be incorporated into the analysis, and, in fact, two recovery measurements with different multiplet spacings can yield both T_1 and T_2. For simple systems, the measured hybrid relaxation time T_{12} is just the weighted average of $R_1 (\equiv T_1^{-1})$ and $R_2 (\equiv T_2^{-1})$:

$$T_{12}^{-1} \equiv R_{12} = pR_2 + qR_1,$$

where p and q are the fractions of time spent in the x-y plane and the z direction, respectively. The formulation is straightforward (Edzes, 1975).

For water in a suspension of red cells, where water molecules exchange between two environments, each with its own (unequal) T_1 and T_2 and with a significant population of nonexchanging protein protons with their own unequal T_1 and T_2, the analysis of a single-scan hybrid relaxation measurement becomes complex. The details will be published elsewhere (Eisenstadt [1]), and we only outline it here, to give all the necessary formulas to extract the cell water lifetime.

We will begin considering relaxation in the T_2 mode. The necessary equations have been presented in the *Measurement and Theory* section, Eqs. (1)–(5*b*).

We first put Eq. 4 in matrix form:

$$\boldsymbol{M}(t) = \tilde{\boldsymbol{C}}(t)\,\boldsymbol{M}_0 \tag{A1}$$

1 M. Eisenstadt. Multiple-pulse methods of studying physical and chemical exchange. *(Submitted for publication).*

where the components of the vector $\boldsymbol{M}_0$ are the initial values in each phase, $[M_{A0}, M_{B0}]$; $\boldsymbol{M}(t)=[M_A(t), M_B(t)]$, and the matrix elements of $\tilde{\boldsymbol{C}}(t)$ are:

$$\begin{aligned}
(\phi_{2+}-\phi_{2-})\,C_{11} &= (k_{2a}+k_x-\phi_{2-})\exp(-\phi_{2+}t) \\
&\quad +(\phi_{2+}-k_{2a}-k_x)\exp(-\phi_{2-}t) \\
(\phi_{2+}-\phi_{2-})\,C_{12} &= -k_y\exp(-\phi_{2+}t)+k_y\exp(-\phi_{2-}t) \\
(\phi_{2+}-\phi_{2-})\,C_{21} &= -k_x\exp(-\phi_{2+}t)+k_x\exp(-\phi_{2-}t) \\
(\phi_{2+}-\phi_{2-})\,C_{22} &= (k_{2b}+k_y-\phi_{2-})\exp(-\phi_{2+}t) \\
&\quad +(\phi_{2+}-k_{2b}-k_y)\exp(-\phi_{2-}t).
\end{aligned} \tag{A2}$$

The F and G phases can be incorporated into the matrix formulation, with a four-component magnetization vector and a four by four relaxation matrix. For T_2, this is a trivial extension; since there is no coupling to the A and B phases [Eq. (2)], it simply adds two diagonal matrix elements. This does not imply that water has no effect on protein T_2, but that protein-proton transverse relaxation does not depend directly on the spin populations of any other phase.

A similar matrix is needed to describe relaxation in the T_1 mode. For pure T_1 experiments, the spin diffusion effects outlined in Eq. (6) must be included. We did develop a three-phase hybrid analysis, but spin transfer effects were much less noticeable because of the short protein T_2. Hence we will restrict the hybrid analysis below to two-phase exchange, which is adequate for almost all cases considered here.

Then for the T_1 portion of the hybrid cycle, we can write a set of rate equations similar to Eq. (2), but the variables are now the deviations of magnetization from thermal equilibrium, $M_A(t)-M_A^0$, etc., and all subscripts are changed from 2 to 1. Their solutions are again of the form of Eqs. (4) and (5), changing 2 to 1. The matrix form is somewhat different, because M is not decaying toward zero:

$$\boldsymbol{M}(t)=\tilde{\boldsymbol{D}}(t)\,\boldsymbol{M}_0+(\mathbf{1}-\tilde{\boldsymbol{D}})\,\boldsymbol{M}^0 \tag{A3}$$

but the matrix elements of $\tilde{\boldsymbol{D}}$ are identical to $\tilde{\boldsymbol{C}}$, Eq. (A2), replacing subscripts 2 by 1.

The result for a hybrid experiment is obtained by successively applying $\tilde{\boldsymbol{C}}$ and $\tilde{\boldsymbol{D}}$ for the time where one or the other is applicable. The relevent times are shown in Fig. 9. First $\tilde{\boldsymbol{C}}$ is applied to the initial $\boldsymbol{M}_0$ for a period τ_2. Using the resultant value $\boldsymbol{M}(\tau_2)$ now as an initial value, $\tilde{\boldsymbol{D}}$ is applied for a time τ_1. Then the cycle is repeated. The state of the magnetization is sampled with a gate close to the first 90° pulse of the τ_2 domain, and we call its value for the

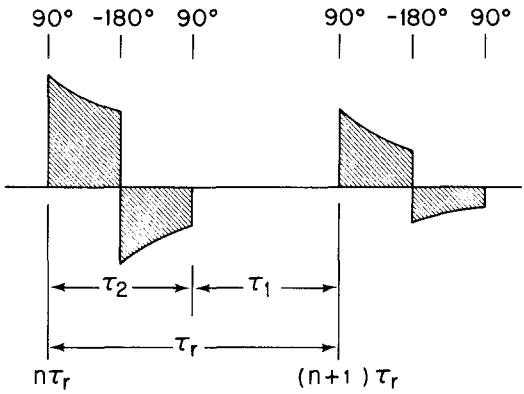

Fig. 9. Basic triplet sequence. Time between the 90° and (−180°) pulse is $\tau_2/2$. Magnetization is in x-y plane during τ_2 and along z direction during τ_1. Sequence repeated every τ_r

n th multiplet $\boldsymbol{M}_n(0)$. The process is continued N times until a constant value $\boldsymbol{M}_\infty(0)$ is reached, be it the equilibrium $\boldsymbol{M}^0$ or not, after which N gates are subtracted in succession from the first N. The measured quantity $\Delta \boldsymbol{M}_n$ is then given by the matrix equation

$$\Delta \boldsymbol{M}_n = \boldsymbol{M}_n(0) - \boldsymbol{M}_\infty(0) = \tilde{\boldsymbol{R}}^n \left(\boldsymbol{M}_0 - \frac{\mathbf{1} - \tilde{\boldsymbol{D}}}{\mathbf{1} - \tilde{\boldsymbol{R}}} \boldsymbol{M}^0 \right) \tag{A4}$$

where we define a relaxation matrix

$$\tilde{\boldsymbol{R}}(\tau_r) = \tilde{\boldsymbol{D}}(\tau_1)\, \tilde{\boldsymbol{C}}(\tau_2). \tag{A5}$$

The solution to Eq. (A4) is derived elsewhere (Eisenstadt [1]) and we only give the final result:

$$\begin{aligned} \Delta M_n = {} & S_+ \exp(-\Phi_+ n\tau_r) + S_- \exp(-\Phi_- n\tau_r) \\ & + S_F \exp(-R_{f12} n\tau_r) + S_G \exp(-R_{g12} n\tau_r) \end{aligned} \tag{A6}$$

with

$$\begin{aligned} \Phi_\pm &= -\ln \lambda_\pm / \tau_r \\ 2\lambda_\pm &= (R_{11} + R_{22}) \pm [(R_{11} - R_{22})^2 + 4R_{12} R_{21}]^{\frac{1}{2}} \\ S_\pm &= \varepsilon_\pm - Q_\pm \\ Q_\pm &= (\kappa_\pm - \delta_\pm)/(1 - \lambda_\pm). \end{aligned} \tag{A7}$$

The matrix elements of $\tilde{\boldsymbol{R}}$ derive from Eqs. (A5) and (A2), where $\tilde{\boldsymbol{C}}$ and $\tilde{\boldsymbol{D}}$ are evaluated for $t = \tau_2$ and τ_1, respectively, and $\tilde{\boldsymbol{D}}$ derives from Eq. (A2) with the subscript change of 2 to 1. The coefficients $\kappa_\pm$, $\varepsilon_\pm$ and $\delta_\pm$ are cumbersome functions of the initial and equilibrium magnetizations, as well

as all of the rates:

$$\begin{aligned}
\kappa_+ &= (M_B^0 - a_- M_A^0)(1 - a_+ a_-)^{-1} \\
\kappa_- &= (M_A^0 - a_+ M_B^0)(1 - a_+ a_-)^{-1} \\
\varepsilon_+ &= (M_{B0} - a_- M_{A0})(1 - a_+ a_-)^{-1} \\
\varepsilon_- &= (M_{A0} - a_+ M_{B0})(1 - a_+ a_-)^{-1} \\
\delta_+ &= [(D_{21} - a_- D_{11}) M_A^0 + (D_{22} - a_- D_{12}) M_B^0](1 - a_+ a_-)^{-1} \\
\delta_- &= [(D_{11} - a_+ D_{21}) M_A^0 + (D_{12} - a_+ D_{22}) M_B^0](1 - a_+ a_-)^{-1} \\
a_- &= (\lambda_- - R_{11})/R_{12} \\
a_+ &= (\lambda_+ - R_{22})/R_{21}.
\end{aligned} \tag{A8}$$

This is the complete solution for the two-phase hybrid experiment, for signal gates narrow compared to any of the R_2^{-1} or ϕ_2^{-1}, and for negligible time between the initial 180° pulse (if any) and the start of the multiplets. We did make some small corrections for these effects, at most one or two percent; formulas are given elsewhere (Eisenstadt [1]). We emphasize that any M_0 can be used as the initial state, even $+M^0$. However, an initial inversion, $-M^0$ gives the largest signal, and is used in the work described above. A numerical analysis of the data using the above is prohibitive by hand, but straightforward to program and used little storage space.

References

Andrasko, J. 1976. Water diffusion permeability of human erythrocytes studied by a pulsed gradient NMR technique. *Biochim. Biophys. Acta* **428**:304

Benga, G., Morariu, V.V. 1977. Membrane defect affecting water permeability in human epilepsy. *Nature (London)* **265**:636

Carr, H.Y., Purcell, E.M. 1954. Effects of diffusion on free precession in nuclear magnetic resonance experiments. *Phys. Rev.* **94**:630

Chien, D.Y., Macey, R.I. 1977. Diffusional water permeability of red cells. Independence on osmolality. *Biochim. Biophys. Acta* **464**:45

Chien, S. 1975. Biophysical behavior of red cells in suspensions. *In:* The Red Blood Cell. Vol. 2. (2nd ed.) D.M. Surgenor, editor. Academic Press, New York

Conlon, T., Outhred, R. 1972. Water diffusion permeability of erythrocytes using an NMR technique. *Biochim. Biophys. Acta* **288**:354

Dick, D.A.T. 1971. Water movement in cells. *In:* Membranes and Ion Transport. Vol. 3. E.E. Bittar, editor. Wiley-Interscience, New York

Edzes, H.T. 1975. An analysis of the use of pulse multiplets in the single scan determination of spin-lattice relaxation rates. *J. Magn. Reson.* **17**:301

Eisenstadt, M., Fabry, M. 1978. NMR relaxation of the hemoglobin-water proton spin system in red blood cells. *J. Magn. Reson.* **29**:591

Fabry, M.E., Eisenstadt, M. 1975. Water exchange between red cells and plasma. Measurement by nuclear magnetic resonance. *Biophys. J.* **15**:1101

Frait, Z., Fraitora, D., Doskocilova, D. 1973. Measurement of the proton NMR field shift in aqueous solutions containing Cu^{2+}, Cr^{3+}, Fe^{3+}, and Mn^{2+} ions. *Czech. J. Phys.* **B 23**:908

Geigy, 1970. Documenta Geigy, Scientific Tables. (7^{th} Ed.) K. Diem and C. Lentner, editors. Geigy Pharmaceuticals, Ardsley, N.Y.

Kuntz, Jr., I.D., Kauzmann, W. 1974. Hydration of proteins and polypeptides. *Adv. Protein Chem.* **28**:239

Meiboom, S., Gill, D. 1958. Modified spin-echo method for measuring nuclear relaxation times. *Rev. Sci. Instrum.* **29**:688

Outhred, R., Conlon, T. 1973. The volume dependence of the erythrocyte water diffusion permeability. *Biochim. Biophys. Acta* **348**:446

Shporer, M., Civan, M.M. 1975. NMR study of ^{17}O from $H_2{}^{17}O$ in human erythrocytes. *Biochim. Biophys. Acta* **385**:81

Solomon, A.K. 1960. Red cell structure and ion transport. *J. Gen. Physiol.* **43 (Suppl. 1–2)**:1

Steck, T.L. 1974. The organization of proteins in the human red blood cell membrane. *J. Cell Biol.* **62**:1

Stein, W.D., 1967. The Movement of Molecules across Cell Membranes. Academic Press, New York

Villegas, R., Barton, T.C., Solomon, A.K. 1958. The entrance of water into beef and dog red cells. *J. Gen. Physiol.* **42**:355

Woessner, D.E. 1961. Nuclear transfer effects in NMR pulse experiments. *J. Chem. Phys.* **35**:41